JOURNAL OF PROPULSION AND POWER
Vol. 18, No. 6, November–December 2002

Measured Flow Oscillations and Instabilities in Labyrinth Seal Cavities

David L. Rhode* and J. Wayne Johnson†
Texas A&M University, College Station, Texas 77843

Two flow instabilities involving a bifurcated flow pattern were discovered for the throughflow jet in a stepped labyrinth seal cavity. These instabilities, along with self-sustained flow oscillations, were experimentally explored to obtain a preliminary understanding of this phenomenon. Computer-captured visualization videos were used to measure the oscillation amplitudes and frequencies, as well as the mean value, of the throughflow jet trajectory angle. It was found that, depending on the seal cavity tooth clearance and radial height of the step, the flow pattern of the throughflow jet leaving the step corner was either 1) nonbifurcated, 2) always bifurcated, or 3) oscillatory bifurcated. A bifurcation stability map was developed showing which combinations of tooth clearance and step height lie in which of the three flow regimes. It was also found that the intermediate value of step height in the presence of the small tooth clearance exhibited the sharpest flow deflection and largest oscillation amplitude, as well as the highest mean-flow leakage resistance. Furthermore, for larger tooth clearances, the large step height cases, located farthest on the stability map into the oscillatory bifurcated regime, gave the highest leakage resistance.

Nomenclature

c	=	tooth radial clearance
K	=	dimensionless leakage resistance coefficient, $2(P_{in} - P_{ex})/\rho U^2$
L	=	streamwise length of open (nonlabyrinth) cavity
M	=	Mach number based on tooth clearance velocity
P_{ex}	=	pressure downstream of seal specimen
P_{in}	=	pressure upstream of seal specimen
Re	=	Reynolds number based on tooth clearance values, $U2c/\nu$
Sr	=	Strouhal number, fc/U
s	=	step height
U	=	bulk velocity at the tooth clearance
W	=	width of open (nonlabyrinth) cavity
θ	=	flow angle at step corner
ν	=	kinematic fluid viscosity
ρ	=	fluid density

Introduction

THE crossflow over an open rectangular cavity is an important type of basic separated flow. Details and parametric influences of such generic flowfields are quite useful in providing an enhanced understanding of fundamental separated flow phenomena. Wall flows tangential to a series of open embedded cavities commonly occur in both external and internal flow situations. Examples of external flow in the aerospace industry include 1) gaps between aircraft skin segments, 2) slots between wings and control surfaces, and 3) numerous gaps between insulating tiles covering the space shuttle. Such flowfields are found in internal flow through 1) fluid machine secondary flow cavities such as those of labyrinth seals, 2) turbine blade internal cooling passages involving surface mounted ribs, and 3) electronic package cooling passages flowing over transistors, etc.

Labyrinth seals in the secondary flowpath of centrifugal compressors and pumps, as well as gas and steam turbines, play an important role in the performance and rotor dynamic arenas. Because of their very high degree of reliability and simplicity, labyrinth seals continue to be the most popular choice in many turbomachinery applications.

The primary objective of labyrinth seals is to restrict fluid flow between regions of high and low pressure by providing a highly frictional flowpath through a series of cavities. An alternative objective is to control internal flow rates of coolant in areas where cooling specific components is vital. A common type of labyrinth seal is the stepped labyrinth, shown in Fig. 1. Such seals are generally used in applications where the use of a contacting seal is inappropriate. Such applications include environments where a contaminant such as dirt particles would cause a contacting seal to wear or fail quickly.

The following section discusses the previous related work. The next two sections consider the test facility and experimental approach. Finally, the results and conclusions are presented.

Previous Work

Concerning seal leakage, at significant leakage Reynolds numbers (approximately 5×10^3–1×10^4) a negligible effect of shaft rotation speed was found by Waschka et al.,[1] Stocker et al.,[2] and others. The limiting Reynolds number, above which shaft speed has little effect, is somewhat dependent on the ratio of swirl to axial velocity. A reasonable conclusion is that, for typical situations, shaft speed has little effect (generally less than 8%) on leakage and heat transfer for fairly large clearances and large pressure drops, that is, where the leakage Reynolds number is fairly high. Concerning labyrinth seal rotor dynamics, however, shaft speed has been found to have a substantial effect. This is particularly true when the seal inlet circumferential velocity component is very different from that of the seal rotor surface.

No data were found in the literature concerning self-sustained flow oscillations in labyrinth seals. However, concerning the related case of the flow across the mouth of an open cavity in general, evidence was found that self-sustaining cavity oscillations are responsible for significant increases in the time mean drag on the body, which for example, houses the cavity. These oscillations can substantially alter the mean velocity distribution of the shear layer, the mean drag on the cavity, and the mean static pressure within the cavity. Measured increases of mean cavity pressure[3] accompanied amplitude increases of an externally excited (using a loudspeaker) oscillation within the cavity. It has been hypothesized that this increase in mean cavity pressure is caused by the presence of a stagnation point during the "suck into the cavity" phase of the freestream during the oscillation cycle. Because of the known enhancement of

Received 20 November 2001; revision received 28 June 2002; accepted for publication 3 July 2002.

*Professor, Mechanical Engineering Department. Member AIAA.
†Graduate Assistant, Mechanical Engineering Department; currently Senior Engineer, Engine Design G217 Dept., Siemens–Westinghouse Power Corporation, Jupiter, Florida 33477.

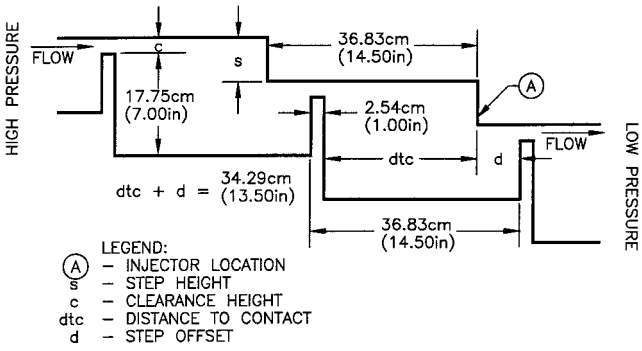

Fig. 1 Stepped labyrinth seal investigated.

the entrainment in free shear layers in the presence of oscillations,[4] it is apparent that the stagnation point moves deeper into the cavity, resulting in further pressure buildup.[5]

A discontinuity in the plot of the cavity-drag coefficient vs Reynolds number occurs at the boundary, which separates shallow ($L/W > 1$) and deep ($L/W < 1$) cavities, as found by Yu.[6] The direction of the dominant wave propagation within shallow and deep cavities is longitudinal and transverse, respectively. Therefore, the drag coefficient discontinuity is not surprising. Further data were reported for long, narrow cavities by Heller and Bliss,[7] who give the cavity-drag coefficient as a function of L/W. It was found that the drag coefficient increases with L/W until L/W reaches 10, after which it decreases. This decrease for large L/W was attributed to the shear layer reattaching to the floor of the cavity.

Self-sustaining, coherent oscillations of impinging shear layers have been observed to cause large unsteady effects in a variety of configurations, including 1) cavities/depressions in submarine and ship hulls, 2) leading tubes in heat exchanger tube bundles, 3) aircraft wheel wells and weapon bays, 4) cavities in gasdynamic lasers, 5) flaps of short takeoff and landing aircraft, and 6) steam regulation and control valves. Several common features among this variety of cavitylike flowfields have resulted in a general framework for describing cavity-flow oscillations.[8] Such oscillations have been classified into three categories: 1) fluid dynamic, in which oscillations occur due to the inherent instability of the flow, 2) fluid resonant, in which oscillations are influenced by the presence of (standing) resonant waves, and 3) fluid elastic, which result from fluid–structure interaction effects, that is, a solid boundary in oscillatory motion. Examples of the fluid dynamic category are characterized by an oscillation frequency that has been traced to the selective amplification of vorticity fluctuations in the cavity shear layer and a feedback mechanism involving the upstream propagation of disturbances, enhanced by the presence of a downstream impingement surface.[8]

For the present study of a very large-scale labyrinth seal, involving rigid surfaces and no compressibility or free-surface effects, the cavity oscillations are of the fluid dynamic category. Early investigators have generally described the nature of the upstream propagation of disturbances as an acoustic or hydrodynamic phenomenon. Experiments have been conducted covering a wide range of conditions: 1) liquid flows by Brackenridge[9] and Rockwell,[10] 2) high-speed airflows by Powell,[11] and 3) low-speed airflows by Powell[12] and Chanaud and Powell.[13]

Two important aspects of such fluid dynamic oscillations, as explained by Rockwell,[14] are the feedback condition and the amplification conditions of the shear layer instability. A necessary, but not sufficient, condition for coherent oscillating flow is the selective amplification characteristic of shear layer flow, causing some disturbances to be amplified more than others. Early investigators have found that the upstream propagation of disturbances (feedback) is enhanced by the presence of the downstream (impingement) cavity surface. This surface propagates pressure perturbation waves upstream, which result in vorticity fluctuations near the sensitive shear layer origin. These fluctuations create amplified disturbances to be further amplified in the shear layer. As implied earlier, the upstream unsteadiness feedback has also been found in the absence of a downstream impingement surface. In either case, the downstream unsteadiness has been attributed by various workers to vortex formation and pairing in mixing layers,[15,16] lateral oscillations of a wake,[17] and change in jet structure at an impingement surface.[18]

Objective

The objective of the present investigation is to explore, for the first time, the effect of the expected presence of self-sustaining flow oscillations, as well as any flow instabilities, on the throughflow jet in a cavity of a stepped labyrinth seal. A stepped labyrinth seal is, in some respects, fairly typical of the throughflow type of cavity found at numerous locations in many turbomachines. A second objective is to obtain a bifurcation flow regime map for these cavities.

Experimental Facility

A closed-loop circulation system was utilized in which water was the working fluid. To provide a nearly constant water temperature, a 2.84-m^3 (750-gal) water storage tank was used. A 3.79-kW (5-hp) centrifugal pump was employed. A 10.16-cm (4-in.) flange-tapped orifice flow meter was located downstream of the test section to measure the volumetric flow rate. The pressure differential across the orifice plate, as well as the seal specimen, was measured with Validyne Model DP 15 variable reluctance pressure transducers.

The nondimensional leakage resistance coefficient K is used to evaluate the leakage performance. This quantity is the minor loss coefficient used to evaluate the frictional energy losses[19] for flow in a pipe or duct bend, for example. Specifically, when comparing two geometries at a given pressure drop ($P_{in} - P_{ex}$), the one exhibiting the higher K value will have the lower mass leakage. This quantity facilitates the comparison of geometry effects without the presence of Reynolds number effects. Seals with low leakage, for a given pressure drop, have a high leakage resistance coefficient. Comparison of seals having a different tooth clearance is possible at high Reynolds number, where the K values tend to be essentially constant.

The test section measures 0.914 m × 2.438 m × 0.914 m (3 ft × 8 ft × 3 ft). It was constructed of welded Hastelloy-X, a corrosion resistant steel alloy. Based on the leakage measurements of Waschka et al.[1] and others, it is known that shaft rotation has little effect on leakage at significant Reynolds numbers, that is, when the ratio of swirl to axial velocity is fairly low. Thus, like most seal leakage test rigs, the rig was designed to provide two-dimensional planar flow, as a sensible approximation to facilitate changes of geometry. However, rotation often has a substantial effect on seal rotordynamics (see "Previous Work" section).

Flow Visualization Equipment

The injected fluorescein dye (diluted with water) was illuminated using an argon-ion laser, Spectra Physics Model 2017 Stabilite, which had a nominal power level of 5 W. The laser beam was directed into the test section using two mirrors, after which it was spread out into a thin sheet, using a quartz rod of diameter 0.635 cm (0.25 in.) as a cylindrical lens. The RCA Pro845 camcorder had a 12× zoom lens with shutter speeds between 60 and 10,000 frames/s. The dye injector tip was located near the stator step corner shown in Fig. 1 at point A. The injector was driven by a pneumatic pressurization system. After experimentation with several different dyes, it was found that fluorescein sodium, acid yellow number 73, from Sigma Chemical Co., was the best with the present laser.

Computer Facilities

For convenience, a 90-MHz Intel® Pentium™-based personal computer with 32-MB RAM, a 2.05-GB Fast small-computer system interface-2 hard disk drive, an Intel Smart Video Recorder PRO™ digital video capture board, and a 128-bit video card with 4-MB VRAM was used to store the visualization movies in digital format. The video capture board is capable of capturing up to 30 frames/s at various screen sizes and compressing the digital information in real time. The 8-mm recording of the experiment is

captured as a full motion video with from 20 to 30 frames/s. The captured digital video is then played back on the computer monitor with a transparent protractor overlay placed on the monitor. The angle at which the throughflow leaves the step separation corner, that is, the flow angle, is read as the center of the mass of dye visible at the arc of the protractor (Fig. 1). The arc radius corresponds to a distance from the step corner of 40% of the cavity depth. The template is correctly scaled to account for camera zoom, etc.

Results

Measurement Uncertainty and Repeatability

The flow rate measurement uncertainty for a given configuration was calculated at approximately 1% using the Kline–McClintock[20] method of uncertainty analysis. The uncertainty for measurement of the leakage resistance coefficient was found to be 3% at typical operating conditions. Furthermore, it was found that the repeatability of the flow angle data taken by the same person on different occasions agreed within 3%. In addition, the repeatability of the same data taken independently by two different observers was determined to agree within 4%. The repeatability measurements quoted here utilize the rms flow angle data. Experimental repeatability of the leakage resistance coefficient was determined to be within 4%.

Preliminary Experiments

The self-sustaining oscillations are trajectory fluctuations of the throughflow jet, an instantaneous digital image of which is shown in Fig. 2a. Several preliminary experiments were conducted to verify that the oscillations and bifurcated flow pattern are not simply due to some type of oscillation from the dye injector system. First, while there was no water flowing through the rig, the injector filled the cavity with dye at a very fast rate and was then turned off; then the water flow was turned on, and self-sustained oscillations, as well as bifurcations of the dye jet (Fig. 2b), were observed. Second, when there was no water flowing through the rig, the dye was turned on at the standard dye flow rate, and no oscillation or bifurcation of the dye jet was observed. Third, while the water was flowing through the rig and the dye supply valve was opened slightly to give the lowest visible dye flow rate, small "blobs" of dye were observed to be intermittently injected into the flowfield, indicating the nature of the oscillating cavity throughflow pressure near location A (Fig. 1). Furthermore, during some time intervals, some of the blobs followed the trajectory of the 45-deg angle at which the injector was mounted at location A, that is, giving the left-hand branch of the dye bifurcation (Fig. 2b), whereas other blobs were dramatically deflected downward toward location 4, shown in Fig. 2a. At other times all of the injected blobs were sharply deflected downward (Fig. 2b), leaving the step corner along a tangent. As the valve was opened to allow a greater dye flow rate, the same phenomenon was observed, except that the dye blobs were darker and larger. Opening the valve further to obtain the standard dye injection rate produced images similar to those in Fig. 2b. In all cases with water flowing through the rig, whether the dye was bifurcated or not, the dye jet exhibited a low-frequency, self-sustained oscillation.

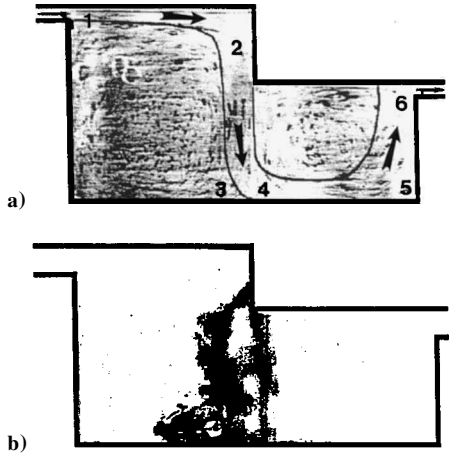

Fig. 2 Typical instantaneous images showing a) throughflow jet time-averaged bounding streamlines (sketched from the author's impression) for clearance c/DTC = 0.037 and step height s/DTC = 0.37 and b) bifurcated flow pattern for clearance c/DTC = 0.15 and step height s/DTC = 0.37 (DTC = 17.15 cm) using injected dye (dark color).

Discussion

After the visualization movies were related to previous work with cavity oscillations, there is little doubt that these oscillations are caused by at least two impingement-feedback phenomena. Moreover, these feedback oscillatory phenomena are probably coupled to some extent. The first of these phenomena is the selective amplification of shear layer instabilities near the cavity inlet tooth (location 1 in Fig. 2a) due to the upstream propagation of vorticity waves as reflections of the vorticity fluctuation impingement on the step wall near location 2. The second impingement feedback is reflected from locations 4 and/or 3, where very large oscillations of the stagnation point location were observed, back to location 2.

The very large-scale seal configurations considered involved the following four tooth clearances: 0.635 (0.25), 1.91 (0.75), 2.54 (1.0), and 3.18 cm (1.25 in.). For each of these clearances, the three step heights considered are 4.45 (1.75), 6.35 (2.5), and 8.26 cm (3.25 in.). One of the intriguing aspects of the stepped seal flowfield is that some configurations exhibit different bifurcation characteristics. A bifurcation stability regime map was developed to illustrate the step height and clearance combinations [normalized by axial displacement distance to contact (DTC) = 17.15 cm (6.75 in.)] for which three distinct flow phenomena were observed. For throughflow Reynolds numbers ($2cU/\nu$) of 3×10^4 and 2×10^4, the regime maps are given in Figs. 3 and 4, respectively. The boundaries separating the three regimes shown were located to pass generally through points in Figs. 3 and 4 at which transitionary behavior was observed. The width of the shading along the boundaries indicates the estimated uncertainty in locating the boundaries. Note that the Reynolds number of 2×10^4 gave greater uncertainty in locating the boundaries. The always bifurcated and oscillatory bifurcated flow patterns were found to be nonbifurcated only about 5% of the time and the nonbifurcated case was bifurcated about 5% of the time. Self-sustained oscillations were observed in all cases, regardless of the presence of bifurcation.

Observe in Fig. 3 that all configurations investigated with a step height less than approximately 5.5 cm (s/DTC = 0.32) gave what the authors have named the nonbifurcated flow pattern. This flow pattern (not shown for brevity) essentially exhibits the expected case of dye leaving the step corner tangentially like the right-hand branch of that in Fig. 2b. The second bifurcation regime is the always bifurcated flow pattern, which was found for step heights greater than 5.5 cm (s/DTC = 0.32) and for intermediate clearances. The images

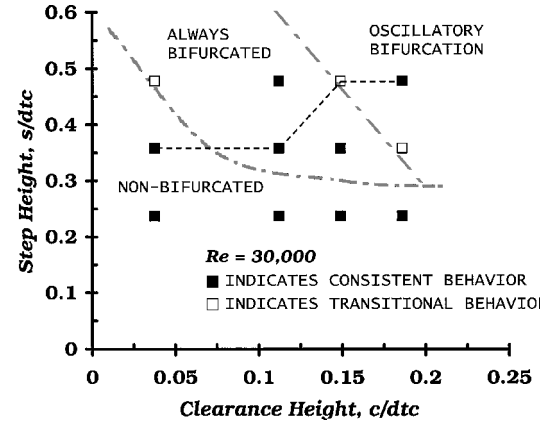

Fig. 3 Stepped labyrinth cavity flow stability map showing the three flow regimes for $Re = 3 \times 10^4$: – – –, highest leakage resistance value for each clearance.

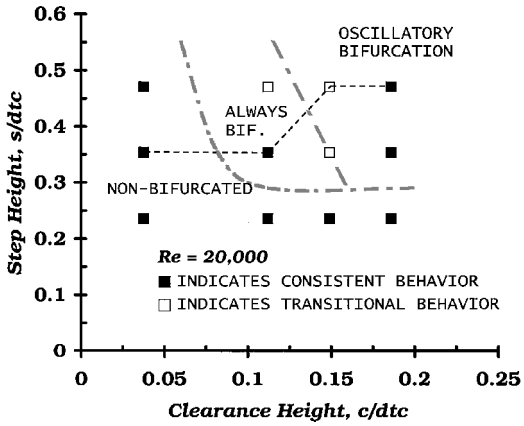

Fig. 4 Stepped labyrinth cavity flow stability map showing the three flow regimes for $Re = 2 \times 10^4$: – – –, highest leakage resistance value for each clearance.

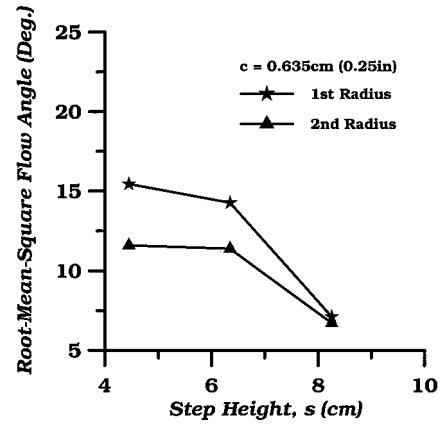

Fig. 6 Measured trajectory flow angle oscillation amplitude (rms) for the three step height cases at tooth clearance c/DTC = 0.037.

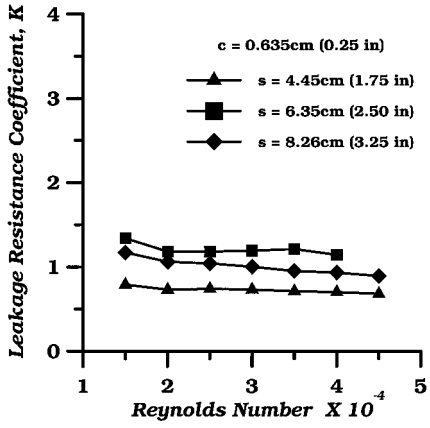

Fig. 5 Measured leakage resistance coefficient for the tooth clearance c/DTC = 0.037 and step heights s/DTC = 0.26, s/DTC = 0.37, and s/DTC = 0.48.

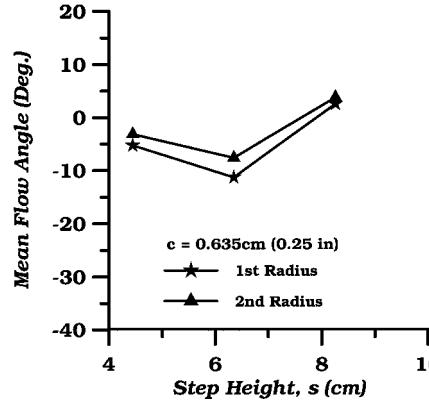

Fig. 7 Measured time mean trajectory flow angle for the three step height cases at tooth clearance c/DTC = 0.037.

showing a bifurcated flow pattern generally show that the left-hand branch is more dominant. The third bifurcation regime was found at large step heights and large clearances. It is named oscillatory bifurcated because it occurs as a random cyclical variation of bifurcated and nonbifurcated flow patterns. To show which regime exhibits the highest leakage resistance for a given tooth clearance, Figs. 3 and 4 include a dashed curve to indicate the highest resistance geometry for each clearance case. For leakage, the clearance is by far the most important design dimension, and thus, each clearance group should be viewed as a distinct category.

Leakage resistance measurements for the three step height cases of smallest tooth clearance, $c = 0.635$ cm, are given in Fig. 5. As the turbulence becomes intense at $Re \approx 2 \times 10^4$, one finds the expected asymptotic invariance of leakage resistance with increasing Reynolds number. The intermediate step height case has the highest resistance, and the large step height case is next. The resistance of the small step height case was expected to be rather poor because of insufficient serpentining of the throughflow jet.

Figure 6 shows the amplitude of the flow oscillation as the rms flow angle θ for the smallest tooth clearance. All of the flow angle data presented in this paper were obtained at a $Re = 3 \times 10^4$. Note that the rms value of 10–15 deg indicates that the magnitude of the throughflow jet oscillation is quite significant. The rms θ value from the first (smaller) radius protractor arc gives a larger oscillation amplitude than that of the second radius for every case considered. This difference is attributed to the intense turbulent diffusion observed between the first and second radii. No major bifurcation of the dye jet was observed here; however, the largest step height case is transitional between nonbifurcated and always bifurcated. The largest step case in Fig. 6 gives a significantly lower rms value than the other step cases. This low value is probably because the longer step surface provides more damping of the dye jet oscillations because the oscillations are perpendicular to the plane comprising the step surface. At the smallest step value, an unusually high rms θ value was found.

The mean values of the dye jet flow angle for the smallest clearance are shown in Fig. 7. Most of the mean θ values are negative because, for some time intervals, the digital images give oscillations with very large negative θ values. Note that the step height case exhibiting the largest leakage resistance ($s = 6.35$ cm) has the most negative mean value of θ and a high oscillation amplitude.

The leakage resistance characteristic for the clearance of 1.91 cm is shown in Fig. 8. Similar to the $c = 0.635$ cm cases, the highest leakage resistance occurs for the intermediate step value, which exhibits the largest rms value and the most negative mean value of θ. Also, like the smallest clearance cases, the large step height here gives the next highest resistance. Not shown for brevity, the mean flow angles are −2, −32, and −5 deg for the small, medium, and large step heights, respectively. In addition, the rms values are approximately 14, 18, and 14 deg for the small, medium, and large step heights, respectively.

The leakage resistance for the $c = 2.54$ cm cases is shown in Fig. 9. The curves have generally the same shape as for the smaller clearance cases. However, a significant difference here is that the highest resistance is found for the largest step height, with the intermediate step giving the next highest value. Like the smaller clearance cases, the intermediate step here has the most negative mean angle and also the largest amplitude. The only detectable distinction from the smaller clearance cases is that the large step case is the only one that is transitioning between the oscillatory bifurcating

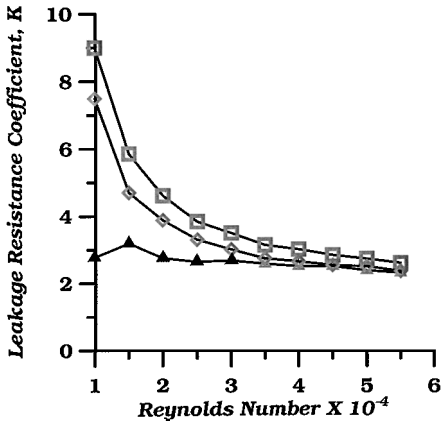

Fig. 8 Measured leakage resistance coefficient for the tooth clearance c/DTC = 0.11 and step heights s/DTC = 0.26, s/DTC = 0.37, and s/DTC = 0.48; c = 1.905 cm (0.75 in.); at s = 4.45 cm (1.75 in.): △, always bifurcated; △, oscillatory bifurcation; and ▲, never bifurcated; at s = 6.35 cm (2.50 in.): □, always bifurcated; □, oscillatory bifurcation; and ■, never bifurcated; and s = 8.26 cm (3.25 in.): ◇, always bifurcated; ◇, oscillatory bifurcation; and ♦, never bifurcated.

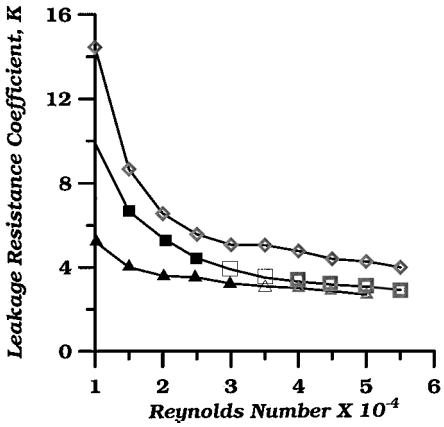

Fig. 9 Measured leakage resistance coefficient for the tooth clearance c/DTC = 0.15 and step heights s/DTC = 0.26, s/DTC = 0.37, and s/DTC = 0.48; c = 2.54 cm (1 in.); at s = 4.45 cm (1.75 in.): △, always bifurcated; △, oscillatory bifurcation; and ▲, never bifurcated; at s = 6.35 cm (2.50 in.): □, always bifurcated; □, oscillatory bifurcation; and ■, never bifurcated; and s = 8.26 cm (3.25 in.): ◇, always bifurcated; ◇, oscillatory bifurcation; and ♦, never bifurcated.

and the always bifurcating regimes near $Re = 2 \times 10^4$ and 3×10^4. The regime boundary is shown in Fig. 9 with a heavy line and has been extrapolated slightly using the dashed curve as shown. Thus, it appears that the fluctuating nature (between the nonbifurcating and the always bifurcating flow patterns) of the oscillatory bifurcation phenomenon is providing enhanced turbulent mixing of high and low momentum fluid to give increased turbulent friction. Furthermore, like the 1.905-cm clearance case, one finds that the 2.54-cm clearance gives no significant change of resistance on transitioning from the nonbifurcating to the always bifurcating regime.

The resistance curves for the largest clearance of $c = 3.175$ cm have a different shape, as shown in Fig. 10. As found for the 2.54-cm clearance cases, the large and the intermediate step heights exhibit the highest and next highest resistance values, respectively. Notice in Fig. 10 that the curves for the small and the intermediate step height have an increased value of resistance for all flow conditions occurring within the oscillatory bifurcation regime. Furthermore, the values for the large step height, which lie farthest into the oscillatory bifurcated regime, are considerably higher than that of the other step heights.

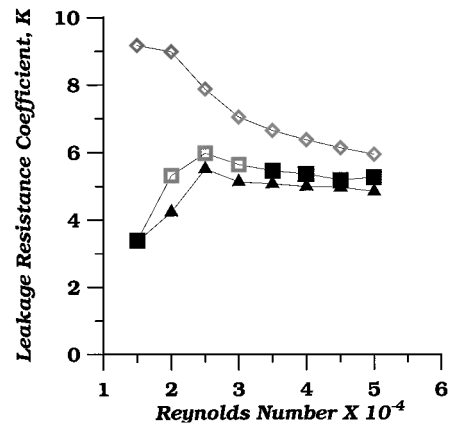

Fig. 10 Measured leakage resistance coefficient for the tooth clearance c/DTC = 0.19 and step heights s/DTC = 0.26, s/DTC = 0.37, and s/DTC = 0.48: c = 3.17 cm (1.25 in.); at s = 4.45 cm (1.75 in.): △, always bifurcated; △, oscillatory bifurcation; and ▲, never bifurcated; at s = 6.35 cm (2.50 in.): □, always bifurcated; □, oscillatory bifurcation; and ■, never bifurcated; and s = 8.26 cm (3.25 in.): ◇, always bifurcated; ◇, oscillatory bifurcation; and ♦, never bifurcated.

Applications

Considering all sizes of gas turbines in general, a wide range of seal geometry (seal clearance, step height, diameter, and DTC) is found operating over a range of conditions (Reynolds number, Mach number, and K). This results in a very wide range of labyrinth seal situations. Specifically, there is a wide range of diameters (approximately from 2.5 cm to 1 m), and each diameter mandates an appropriate radial clearance for its labyrinths. Furthermore, the clearance, pressure drop, and flow conditions result in a Reynolds number, Mach number, and K occurring over a very wide range. Typical ranges for the geometry and operating parameters for gas turbines are estimated as $0.01 < c/\mathrm{DTC} < 0.6$, $0.01\ s/\mathrm{DTC} < 1.0$, $2 \times 10^3 < Re < 1 \times 10^5$, $0.1 < M < 1.0$, $0.1 < K < 15$, and $0 < V_{\mathrm{cir}}/R\omega < 2.0$.

The flow oscillations and bifurcated flow pattern described herein are expected to occur in actual engine seals. The present results may be easily scaled from the very-large-scale test rig to essentially any reasonably sized labyrinth using reasonable caution. Because the present results are taken from water flow, it is anticipated that they are realistic for seal applications at Mach numbers below 0.5 or perhaps 0.4, that is, small density change. Furthermore, the effect on seal leakage of the circumferential velocity entering the seal (zero for the present results) and the shaft peripheral speed are generally less than 8%. However, the ratio of seal inlet circumferential velocity to shaft peripheral speed ($V_{\mathrm{circ}}/R\omega$) is extremely important for seal rotor dynamic forces exerted on the rotor by the fluid in the seal. Although an improved understanding of the self-excited seal rotor dynamics has recently been obtained through computational fluid dynamics-perturbation modeling,[21] a great deal more information is necessary to estimate the possibility of interaction between the oscillatory bifurcation phenomenon and the rotor dynamic instability of labyrinths seals. The oscillations occur over a wide range of frequencies in the current water flow. In terms of the Strouhal number Sr, they span the frequency range of approximately $0.01 < Sr < 0.3$.

Summary

Two flow instabilities involving a bifurcation flow pattern were discovered at the land step separation corner (near the injector location A in Fig. 1) of the seal cavity and coexist with significant self-sustaining flow oscillations. Numerous flow visualization experiments were conducted to obtain an enhanced understanding of the instabilities and oscillations. A bifurcation regime map was constructed, giving which combinations of tooth clearance and step height lie within which of the three bifurcation flow regimes. The following list summarizes the findings.

1) For cavity step heights less than 5.5 cm ($s/\mathrm{DTC} = 0.32$), regardless of tooth clearance, no bifurcation of the throughflow jet was found.

2) For step heights greater than 5.5 cm combined with intermediate values of tooth clearance, the throughflow jet was generally always bifurcated.

3) For large step heights combined with large tooth clearances, an oscillatory bifurcation flow pattern was found.

4) For tooth clearances less than or equal to 1.91 cm ($c/\mathrm{DTC} = 0.11$), the throughflow trajectory is quite important. The step height case giving the highest leakage resistance exhibits a) the most negative mean value of θ and b) cavity oscillations of very large amplitude.

5) For tooth clearances greater than or equal to 2.54 cm ($c/\mathrm{DTC} = 0.15$), the oscillating nature of the oscillatory bifurcation flow pattern appears to exhibit a contribution toward increased leakage resistance via enhanced turbulent mixing.

Acknowledgments

The authors are grateful for the financial support received from the NASA Center for Space Power and the Texas Advanced Technology Program. In addition, we greatly appreciate the contribution of L. Chavez in reading the flow angles.

References

[1]Waschka, W., Wittig, S., and Kim, S., "Influence of High Rotational Speeds on the Heat Transfer and Discharge Coefficients in Labyrinth Seals," *Journal of Turbomachinery*, Vol. 114, No. 2, 1992, pp. 462–468.

[2]Stocker, H. L., Cox, D. M., and Holle, G. F., "Aerodynamic Performance of Conventional and Advanced Design Labyrinth Seals with Solid-Smooth, Abradable, and Honeycomb Lands," Detroit Diesel Allison, Div. of General Motors Corp., Indianapolis, IN, NASA Contract NAS 3-20056, 1977.

[3]Kovasznay, L. S. G., and Ho, C.-M., "Static Pressure Rise in Acoustically Driven Cavities," *AIAA Journal*, Vol. 13, No. 10, 1975, pp. 1403–1404.

[4]Rockwell, D., "Transverse Oscillations of a Jet in a Jet-Splitter System," *Journal of Basic Engineering*, Vol. 94, No. 3, 1972, pp. 675–681.

[5]Rockwell, D., and Naudascher, E., "Review—Self-Sustaining Oscillations for Flow Past Cavities," *Journal of Fluids Engineering*, Vol. 100, No. 2, 1978, pp. 154–165.

[6]Yu, Y. H., "Measurements of Sound Radiation from Cavities at Subsonic Speeds," *Journal of Aircraft*, Vol. 14, No. 9, 1977, pp. 838–843.

[7]Heller, H., and Bliss, D., "Aerodynamically Induced Pressure Oscillations in Cavities: Physical Mechanisms and Suppression Concepts," U.S. Air Flight Dynamics Lab., AFFDL-TR-74-133, 1975.

[8]Naudascher, E., "From Flow Stability to Flow-Induced Excitation," *Proceedings of the ASCE, Journal of the Hydraulics Division*, Vol. 93, 1967, pp. 15–40.

[9]Brackenridge, J. B., "Transverse Oscillation of a Liquid Jet," *Journal Acoustical Society of America*, Vol. 32, No. 10, 1960, pp. 1237–1242.

[10]Rockwell, D., "External Excitation of Planar Jets," *Journal of Applied Mechanics*, Vol. 39, No. 4, 1972, pp. 883–890.

[11]Powell, A., "On Edgetones and Associated Phenomena," *Acoustica*, Vol. 3, 1953, pp. 233–243.

[12]Powell, A., "On the Edgetone," *Journal Acoustic Society of America*, Vol. 33, No. 4, 1961, pp. 395–409.

[13]Chanaud, R. D., and Powell, A., "Some Experiments Concerning the Hole and Ring Tone," *Journal Acoustical Society of America*, Vol. 37, No. 5, 1965, pp. 902–911.

[14]Rockwell, D., "Oscillations of Impinging Shear Layers," *AIAA Journal*, Vol. 21, No. 5, 1983, pp. 645–664.

[15]Dimotakis, P. E., and Brown, G. L., "The Mixing Layer at High Reynolds Number: Large-Structure Dynamics and Entrainment," *Journal of Fluid Mechanics*, Vol. 78, Pt. 3, 1976, pp. 535–560.

[16]Rockwell, D., and Knisely, C., "The Organized Nature of Flow Impingement Upon a Corner," *Journal of Fluid Mechanics*, Vol. 93, Pt. 3, 1979, pp. 413–432.

[17]Tam, C. K. W., "Discrete Tones of Isolated Airfoils," *Journal of the Acoustical Society of America*, Vol. 55, No. 6, 1974, pp. 1173–1177.

[18]Horne, C., and Karamcheti, K., "Some Features of Wall Jet Tones," AIAA Paper 79-0606, 1979.

[19]Fox, R. W., and McDonald, A. T., *Introduction to Fluid Mechanics*, 3rd ed., Wiley, New York, 1985, pp. 359–395.

[20]Kline, S. J., and McClintock, F. A., "Describing Uncertainties in Single-Sample Experiments," *Mechanical Engineering*, Vol. 75, No. 1, 1953, pp. 3–9.

[21]Kim, N., Park, S.-Y., and Rhode, D. L., "Predicted Effects of Shunt Injection on the Rotordynamics of Gas Labyrinth Seals," *Journal of Engineering for Gas Turbines and Power* (to be published); also American Society of Automotive Engineers, ASME Paper 2001-GT-239, 2001.